

Pion transverse-momentum spectrum and elliptic anisotropy of partially coherent source

Peng Ru^{1,*}, Ghulam Bary^{1,†}, and Wei-Ning Zhang^{1,2,‡}

¹*School of Physics, Dalian University of Technology, Dalian, Liaoning 116024, China*

²*Department of Physics, Harbin Institute of Technology, Harbin, Heilongjiang 150006, China*

We study the pion momentum distribution of a coherent source and investigate the influences of the coherent emission on pion transverse-momentum spectrum and elliptic anisotropy. With a partially coherent source, constructed by conventional viscous hydrodynamic model and a parameterized coherent source model, we reproduce the pion transverse-momentum spectrum and elliptic flow in the peripheral Pb-Pb collisions at $\sqrt{s_{NN}} = 2.76$ TeV. It is found that the influences of coherent emission on pion transverse-momentum spectrum and elliptic flow are related to the initial size and shape of the coherent source. This is a quantum effect but not from source dynamical evolution. The results of the partially coherent source with 33% coherent emission and 67% hydrodynamic chaotic emission are consistent with the experimental measurements of pion transverse-momentum spectrum, elliptic flow, and four-pion Bose-Einstein correlations.

PACS numbers: 25.75.Gz, 25.75.Ld, 25.75.Dw

I. INTRODUCTION

Particle transverse-momentum spectrum and elliptic flow are important observables in relativistic heavy-ion collisions [1–8]. By examining particle transverse-momentum spectrum one can obtain the information of the thermalization and expansion of the particle-emitting sources produced in the collisions [1–5, 9]. And, particle azimuthal anisotropic flow is related to the source initial anisotropic pressure gradient [6–8, 10–12], viscosity [13–19], the uncertainty relation of quantum mechanics [20], and even the particle escape from spatially asymmetric source [21].

Recently, ALICE Collaboration observe a significant suppression of three- and four-pion Bose-Einstein correlations in the Pb-Pb collisions at $\sqrt{s_{NN}} = 2.76$ GeV at the Large Hadron Collider (LHC) [22, 23]. This may indicate that there is a considerable degree of coherent emission of pion in relativistic heavy-ion collisions [22–27]. Besides the pion Bose-Einstein condensation [24–26, 28], pion laser [29], disoriented chiral condensate (DCC) [30–33], gluonic condensate [34–36], and even the initial-stage coherent gluon field [37–39] may possibly lead to coherent particle emissions in relativistic heavy-ion collisions. It is meaningful to explore the effects of particle coherent emission on the final-state observables.

The effect of Bose-Einstein condensation on the particle velocity distribution has been observed in ultra-cold atomic gases [40, 41]. The appearing of condensate leads to a decrease of the velocity distribution width. Because the frequencies ω_i of the trapping potential (thus the trapping size $a_i \sim \sqrt{1/\omega_i}$ [25]) are different in the symmetry-axis direction and the directions perpendicular to the symmetry-axis direction, the two-dimension velocity distribution presents elliptical pattern when the condensate appearing [40, 41]. This is a response of quantum mechanics to the asymmetric spatial configuration of the condensate. The investigation of the analo-

gous particle momentum (velocity) anisotropic distribution in relativistic heavy-ion collisions is of great interest for exploring the origin of coherence of the particle-emitting source.

In this paper, we shall study the pion momentum distribution and azimuthal anisotropy of the coherent and chaotic emissions in relativistic heavy-ion collisions. We shall investigate the influences of source geometry and expansion on the pion transverse-momentum spectrum and the elliptic anisotropy (elliptic flow). We shall construct a partially coherent pion source combined with a hydrodynamic chaotic source and a parameterized coherent source and compare the results of the pion transverse-momentum spectrum and elliptic flow of the partially coherent source with the experimental data of the Pb-Pb collisions at $\sqrt{s_{NN}} = 2.76$ TeV at the LHC. It is found that the influences of coherent emission on pion transverse-momentum spectrum and elliptic anisotropy are related to the initial size and shape of the coherent source. The results of the partially coherent source with 33% coherent emission and 67% hydrodynamic chaotic emission are consistent with the experimental measurements of pion transverse-momentum spectrum, elliptic flow, and four-pion Bose-Einstein correlations.

The rest of this paper is organized as follows. In Sec. II, we present the formulas of momentum distributions for the pion coherent and chaotic emissions. In Sec. III, we calculate the effects of source geometry and expansion on pion transverse-momentum spectrum and elliptic flow. In Sec. IV, the results of the partially coherent source are presented and compared with the experimental data at the LHC. Finally, we give the summary and discussion in Sec. IV.

II. PION MOMENTUM DISTRIBUTION FOR COHERENT AND CHAOTIC EMISSIONS

A well known purely coherent multi-particle system is the radiation field of classical source (current) [42–46]. In this model, the final state of the pion field produced by a classical

*Electronic address: pengru@mail.dlut.edu.cn

†Electronic address: ghulamabary@mail.dlut.edu.cn

‡Electronic address: wnzhang@dlut.edu.cn

source $\rho(x) = \rho(t, \mathbf{r})$ can be written as [46]

$$|\phi_\pi\rangle = e^{-\bar{n}/2} \exp\left(i \int d^3p \mathcal{A}(\mathbf{p}) a^\dagger(\mathbf{p})\right) |0\rangle, \quad (1)$$

where $a^\dagger(\mathbf{p})$ is the pion creation operator for momentum \mathbf{p} , $\mathcal{A}(\mathbf{p})$ is an amplitude related to the on-shell ($E_p^2 = \mathbf{p}^2 + m_\pi^2$) Fourier transform of $\rho(x)$,

$$\mathcal{A}(\mathbf{p}) = A(\mathbf{p}) \tilde{\rho}(\mathbf{p}) = A(\mathbf{p}) \int d^4x e^{i(E_p t - \mathbf{p} \cdot \mathbf{r})} \rho(t, \mathbf{r}), \quad (2)$$

$$A(\mathbf{p}) = \left[2E_p(2\pi)^3\right]^{-1/2}, \quad (3)$$

and

$$\bar{n} = \int d^3p |\mathcal{A}(\mathbf{p})|^2 \quad (4)$$

is the average pion number in the final state.

Considering $|\phi_\pi\rangle$ is an eigenstate of the annihilation operators $a(\mathbf{p})$, we can write the single-pion momentum distribution by

$$P_c(\mathbf{p}) = \text{Tr}\left[D_\pi a^\dagger(\mathbf{p}) a(\mathbf{p})\right] = |\mathcal{A}(\mathbf{p})|^2 = A(\mathbf{p})^2 |\tilde{\rho}(x)|^2, \quad (5)$$

where $D_\pi = |\phi_\pi\rangle\langle\phi_\pi|$ is density matrix. An important property of the coherent state $|\phi_\pi\rangle$ is that the multi-pion momentum distribution can be factorized into the product of the single-pion momentum distributions,

$$P_c(\mathbf{p}_1, \dots, \mathbf{p}_m) = \text{Tr}\left[D_\pi a^\dagger(\mathbf{p}_1) \cdots a^\dagger(\mathbf{p}_m) a(\mathbf{p}_m) \cdots a(\mathbf{p}_1)\right] \\ = |\mathcal{A}(\mathbf{p}_1)|^2 \cdots |\mathcal{A}(\mathbf{p}_m)|^2. \quad (6)$$

In order to distinguish with the amplitude and source density of the chaotic pion emission, which will be discussed later, we shall use the denotations $A_c(\mathbf{p})$, $\rho_c(x)$, and $\tilde{\rho}_c(\mathbf{p})$ for the source of the coherent state.

For chaotic pion emission, the single-pion momentum distribution is the superposition of the momentum distributions for all source points, because each of the source point emits pion independently,

$$P_\chi(\mathbf{p}) = \sum_i P_\chi^i(\mathbf{p}) = \sum_i |A_\chi^i(\mathbf{p})|^2 = \int d^4x \rho_\chi(x) A_\chi(x, \mathbf{p})^2, \quad (7)$$

where $\rho_\chi(x)$ is the chaotic source distribution. The two- and multi-pion momentum distributions cannot be expressed as the product of the single-pion momentum distributions. This leads to the so-called HBT correlations [47, 48].

Assuming that all the sub-sources in the chaotic source emit pion thermally at a same freeze-out temperature T_f , we have for a static source,

$$P_\chi(\mathbf{p}) = A_\chi(\mathbf{p})^2 \sim \frac{1}{e^{E_p/T_f} - 1}. \quad (8)$$

We can see that in this case the single-pion momentum distribution for chaotic source is independent of the source space-time distribution. However, the single-pion momentum distribution for coherent source depends on the source space-time distribution,

$$P_c(\mathbf{p}) = A_c(\mathbf{p})^2 |\tilde{\rho}_c(\mathbf{p})|^2 \sim \frac{1}{E_p} |\tilde{\rho}_c(\mathbf{p})|^2. \quad (9)$$

Generally speaking, the particle momentum distribution of evolving sources will be affected by the source geometry and expansion. Next, we shall examine the effects of source anisotropic geometry and expanding velocity on pion transverse-momentum spectrum and elliptic anisotropy for evolving coherent and chaotic sources.

III. EFFECTS OF SOURCE ANISOTROPIC GEOMETRY AND EXPANSION ON PION MOMENTUM SPECTRUM AND ELLIPTIC ANISOTROPY

To make some quantitative comparisons between the effects of coherent and chaotic emissions on pion transverse-momentum spectrum and elliptic anisotropy, we perform a source parametrization for both of the coherent and chaotic sources. In relativistic heavy-ion collisions, the source expansion in transverse plane (xy -plane) is anisotropic due to the anisotropic transverse distribution of the energy deposition in the nuclear overlap zone. We consider an evolving source with a Gaussian initial spatial distribution in the source center-of-mass frame (CMF) as,

$$\rho_{i-s}(\mathbf{r}_0) = \frac{(R_x R_y R_z)^{-1}}{\sqrt{(2\pi)^3}} \exp\left(-\frac{x_0^2}{2R_x^2} - \frac{y_0^2}{2R_y^2} - \frac{z_0^2}{2R_z^2}\right), \quad (10)$$

where R_x , R_y , and R_z represent the spatial sizes of the source at an initial time t_0 . Then, we assume that each of the source element has an expanding velocity in the CMF as [49, 50]

$$v_j(\mathbf{r}_0) = \text{sign}(r_{0j}) \cdot a_j \left(\frac{|r_{0j}|}{R_{j,max}}\right)^{b_j}, \quad (11)$$

where $j = x, y, \text{ or } z$ denotes the velocity component and $\text{sign}(r_{0j}) = \pm 1$ for positive/negative r_{0j} ensuring the source being expansive. The magnitude of v_j increases with $|r_{0j}|$, and the rate of the increase is decided by the positive parameters a_j , b_j and $R_{j,max}$. In our calculations, we take $R_{j,max} = 3R_j$, and consider the source with $|v| < 1$.

The temporal distribution of each source element in its local rest frame (LRF) is parameterized to be a Gaussian distribution with the duration time τ'_s . Thus the space-time distribution of a source element can be written in the LRF as

$$\rho'(x') = \sqrt{\frac{2}{\pi}} \tau_s'^{-1} \exp\left[-\frac{(t' - t'_0)^2}{2\tau_s'^2}\right] \delta^{(3)}(\mathbf{r}'), \quad (t' > t'_0). \quad (12)$$

With Eqs. (10), (11), and (12), we complete the parametrization for both of the coherent and chaotic sources.

The Lorentz invariant momentum distributions of the evolving coherent and chaotic sources are given by the integrals over all particle-emitting source points,

$$E_p P_c(\mathbf{p}) = E_p \left| \int d^4x e^{ip \cdot x} \rho(x) A_c(x, \mathbf{p}) \right|^2, \quad (13)$$

and

$$E_p P_\chi(\mathbf{p}) = E_p \int d^4x \rho(x) A_\chi(x, \mathbf{p})^2. \quad (14)$$

Considering all particle-emitting source points are evolved from the initial source, we can write the source distribution as

$$\rho(x) = \int d\mathbf{r}_0 \rho_{i-s}(\mathbf{r}_0) \rho_0(x), \quad (15)$$

where $\rho_0(x)$ is the source density in the CMF contributed by the initial source element at \mathbf{r}_0 . Using the coordinates \tilde{x} in the CMF with spatial origin point at the \mathbf{r}_0 instead of x , $\mathbf{r} = \mathbf{r}_0 + \tilde{\mathbf{r}}$, $t = \tilde{t}$, there are $\rho_0(x) = \rho_0(\tilde{x})$ and $A_{c/\chi}(x, \mathbf{p}) = A_{c/\chi}(\tilde{x}, \mathbf{p})$. Then, we have from Eqs. (13), (14), and (15),

$$E_p P_c(\mathbf{p}) = E_p \left| \int d\mathbf{r}_0 \rho_{i-s}(\mathbf{r}_0) e^{-i\mathbf{p} \cdot \mathbf{r}_0} \mathcal{A}_{c_0}(\mathbf{p}) \right|^2, \quad (16)$$

$$E_p P_\chi(\mathbf{p}) = E_p \int d\mathbf{r}_0 \rho_{i-s}(\mathbf{r}_0) \mathcal{A}_{\chi_0}(\mathbf{p})^2, \quad (17)$$

where

$$\mathcal{A}_{c_0}(\mathbf{p}) = \int d^4\tilde{x} e^{ip \cdot \tilde{x}} \rho_0(\tilde{x}) A_c(\tilde{x}, \mathbf{p}), \quad (18)$$

$$\mathcal{A}_{\chi_0}(\mathbf{p})^2 = \int d^4\tilde{x} \rho_0(\tilde{x}) A_\chi(\tilde{x}, \mathbf{p})^2. \quad (19)$$

From Eqs. (8) and (9), the amplitudes in the LRF are functions of E'_p , $A'_{c/\chi}(\mathbf{p}') = A'_{c/\chi}(E'_p)$. It is convenient to calculate $\mathcal{A}_{c_0}(\mathbf{p})$ and $\mathcal{A}_{\chi_0}(\mathbf{p})$ in the LRF. Noting

$$\sqrt{E_p} A_{c/\chi}(x, \mathbf{p}) = \sqrt{E'_p} A'_{c/\chi}(E'_p), \quad (20)$$

we have

$$\begin{aligned} \mathcal{A}_{c_0}(\mathbf{p}) &= \frac{1}{\sqrt{E_p}} \frac{\tau_s^{-1}}{\sqrt{2^3 \pi^2}} \int_{t'_0}^{\infty} dt' \exp \left[iE'_p(t' - t'_0) - \frac{(t' - t'_0)^2}{2\tau_s^2} \right] \\ &\equiv \frac{1}{\sqrt{E_p}} G_0(E'_p) = \frac{1}{\sqrt{E_p}} G_0[(\mathbf{p} \cdot \mathbf{u})], \end{aligned} \quad (21)$$

and

$$\mathcal{A}_{\chi_0}(\mathbf{p}) = \frac{1}{\sqrt{E_p}} \sqrt{E'_p} A'_\chi(E'_p) = \frac{\sqrt{(\mathbf{p} \cdot \mathbf{u})}}{\sqrt{E_p}} A'_\chi[(\mathbf{p} \cdot \mathbf{u})], \quad (22)$$

where \mathbf{u} is the 4-velocity of the particle-emitting source points.

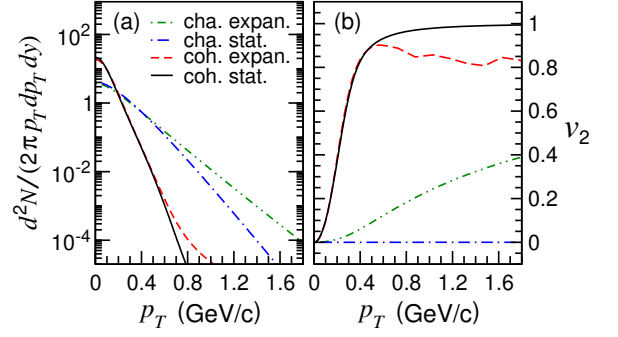


FIG. 1: (Color online) Pion transverse-momentum spectrum (left panel) and the second-order azimuthal anisotropic coefficient $v_2(p_T)$ (right panel) for the static/expanding coherent and chaotic sources with the initial geometry parameters $R_T = R_z = 1$ fm, $S_T = 2$, and $\tau_S = 3$ fm/c. The velocity parameters for the expanding sources are taken to be $a_x = 0.6$, $a_y = 0.4$, $a_z = 0.5$, and $b_{x,y,z} = 0.5$. The temperature of the chaotic source is 100 MeV.

We plot in Fig. 1 the pion transverse-momentum spectrum at central rapidity and the elliptic anisotropy, $v_2(p_T) = \langle (p_x^2 - p_y^2)/p_T^2 \rangle$, for the static/expanding coherent and chaotic sources. Here, the initial transverse and longitudinal spatial size parameters are taken to be $R_T \equiv \sqrt{R_x R_y} = R_z = 1$ fm, the initial transverse shape parameter is taken to be $S_T \equiv R_y/R_x = 2$, the duration time in CMF τ_s is taken to be 3 fm/c, and the velocity parameters for the expanding sources are taken to be $a_x = 0.6$, $a_y = 0.4$, $a_z = 0.5$, and $b_{x,y,z} = 0.5$, respectively. The temperature of the chaotic source is 100 MeV. The source expansion velocity increases the width of transverse-momentum distribution for chaotic emission. This velocity effect for the coherent source is small. Because $\mathcal{A}_{c_0}(\mathbf{p})$ is independent of the spatial coordinate \mathbf{r}_0 for the static coherent source, we have $P_c(\mathbf{p}) \sim \exp(-R_x^2 p_x^2 - R_y^2 p_y^2 - R_z^2 p_z^2)$. The v_2 increases with p_T and approaches to 1 at high p_T [$v_2 = I_1(p_T^2(R_y^2 - R_x^2)/2)/I_0(p_T^2(R_y^2 - R_x^2)/2)$]. For the expanding sources, the v_2 of the coherent source decreases in $p_T > 0.5$ GeV/c region, while the anisotropic expansion velocity leads to the nonzero v_2 for the chaotic emission.

Unlike the elliptic flow of the chaotic source, which is caused by the anisotropic transverse expansion of the source, the v_2 of the coherent source arises from the initial geometry of the source. This is a quantum effect and the value of v_2 will be changed somewhat by the source expansion. To examine the quantum effect we compare in Fig. 2 the results of the transverse-momentum spectrum and v_2 for the expanding coherent sources with the different initial geometry parameters $R_T = 0.2, 0.5$, and 1.0 fm. In the calculations R_z is taken as the same as R_T and the other parameters are the same as in Fig. 1. One can observe that the transverse-momentum spectrum for small R_T increases at high p_T because of a wider distribution of the particle momentum for a smaller source size. The increase of v_2 with p_T covers a larger range for smaller R_T than that for larger R_T .

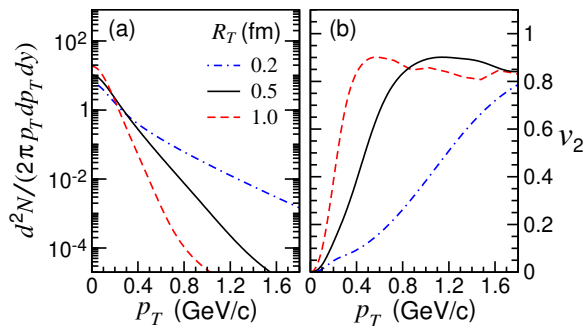


FIG. 2: (Color online) Pion transverse-momentum spectrum (left panel) and the second-order azimuthal anisotropic coefficient $v_2(p_T)$ (right panel) for the expanding coherent sources with the initial geometry parameters $R_T = 0.2, 0.5,$ and 1.0 fm. In the calculations R_z is taken as the same as R_T and the other parameters are the same as in Fig. 1.

IV. RESULTS OF PARTIALLY COHERENT SOURCE

As we have seen in the last section, the v_2 of the coherent source is quantum effect but not from source dynamical evolution. It is different from that of chaotic source. Meanwhile, the transverse-momentum spectrum will be affected by the initial geometry of the coherent source. In high-energy heavy-ion collisions, the created pion source is possibly partially coherent [51]. The significant suppression of multi-pion Bose-Einstein correlations observed by the ALICE collaboration recently in the Pb-Pb collisions at the LHC [22, 23] indicates that the pion emission may have a considerable degree of coherence. In this section, we shall investigate the pion transverse-momentum spectrum and elliptic flow in a partially coherent source model.

For a partially coherent source, the single pion momentum distribution can be written as [52]

$$P(\mathbf{p}) = \left| \sum_x^c |A_c(\mathbf{p}, x)| e^{i\phi_c(x)} e^{i\mathbf{p}\cdot\mathbf{x}} + \sum_x^\chi |A_\chi(\mathbf{p}, x)| e^{i\phi_\chi(x)} e^{i\mathbf{p}\cdot\mathbf{x}} \right|^2, \quad (23)$$

where ϕ_c and ϕ_χ represent the phases of coherent and chaotic emissions, and \sum^c and \sum^χ denote the sums over all the coherent and chaotic source points respectively. By expanding the absolute square of the amplitude and casting out the terms with the random chaotic phase $\phi_\chi(x)$, which can be cancelled each other out and give negligible contribution, we have

$$\begin{aligned} P(\mathbf{p}) &= \left| \sum_x^c A_c(\mathbf{p}, x) e^{i\mathbf{p}\cdot\mathbf{x}} \right|^2 + \sum_x^\chi |A_\chi(\mathbf{p}, x)|^2 \\ &= P_c(\mathbf{p}) + P_\chi(\mathbf{p}). \end{aligned} \quad (24)$$

Because there is no interference effect between the coherent and chaotic emissions in the single momentum distribution, the pion transverse-momentum spectrum and elliptic flow are the sums of the contributions of the coherent and chaotic sources.

We construct a partially coherent pion source as following.

(1) For the chaotic part, we adopt the viscous hydrodynamic code in the iEBE-VISHNU code package [53], which is widely used in the study of relativistic heavy-ion collisions. To be specific, we use the MC-KLN model for the initial condition based on the ideas of parton saturation in the CGC [54, 55]. For one studied centrality class, we use a smooth single-shot initial condition [53, 56], obtained by averaging 1000 randomly generated events with the maximum specified eccentricity, as the input of the hydrodynamical evolution. Since at this step we don't focus on the effects of the event-by-event fluctuations, the single-shot event, which carries the main feature of the chaotic source, is economical for our simulation. With the initial condition prepared, we perform the (2+1)-dimensional viscous hydrodynamics code VISHNew, an improved version of VISH2+1 [57–59] incorporating the lattice QCD-based equation of state s95p-PCE [60], to evolve the source. We set the initial time of the hydrodynamical evolution at $\tau_0 = 0.6$ fm/c and the decoupling temperature at $T_{\text{dec}} = 120$ MeV, which is the same as used in Ref. [17]. After the Cooper-Frye procedure [61], we obtain the pion momentum distribution for the hydrodynamic (chaotic) source by utilizing the AZHYDRO resonance decay code [62–64].

(2) For the coherent part, because the real mechanism responsible for the coherent pion production is not clear so far, we adopt the parameterized expanding source as introduced in the last Section. The initial source spatial distribution is a Gaussian one as Eq. (10), the source expansion velocity is described by Eq. (11), and the temporal distribution is given by Eq. (12).

(3) For simplicity, we considered an idealization that the chaotic and coherent sources evolve independently in the partially coherent source model.

From the measurements of four-pion Bose-Einstein correlation functions in the Pb-Pb collisions at $\sqrt{s_{NN}} = 2.76$ TeV [23], the coherent fraction is about 30% and has not obvious centrality dependence. On the other hand, the observed suppression on the correlations extends at least up to $p_T \sim 340$ MeV/c [23]. So, we estimate the initial (minimum) transverse size of coherent emission region is $\lesssim \hbar/(2 \times 340 \text{ MeV}/c) = 0.29$ fm.

In the left and middle panels of Fig. 3, we show the results of pion transverse momentum spectrum and elliptic flow, respectively, for the Pb-Pb collisions at $\sqrt{s_{NN}} = 2.76$ TeV and in 40–50% centrality region. Here, the blue dashed lines and squares are the results of the hydrodynamic chaotic source with the ratio of shear viscosity to entropy density $\eta/s = 0.20$ [17]. The red solid lines and circles are the results of the partially coherent source constructed with the hydrodynamic chaotic source with $\eta/s = 0.43$ and the coherent source with the initial geometry parameter $R_T = R_z = 0.25$ fm. The duration time and expansion velocity parameters for coherent source are taken to be $\tau_s = 2$ fm, $a_x = 0.4$, $a_y = 0.3$, and $a_z = 0.35$, and the other parameters are the same as in the last section. For the partially coherent source, the total fractions of chaotic and coherent emissions, obtained with the particle yields in the transverse momentum range $p_T < 3$ GeV/c, are 67% and 33%, respectively. In these panels, the black bullets are the experimental data of the transverse-momentum

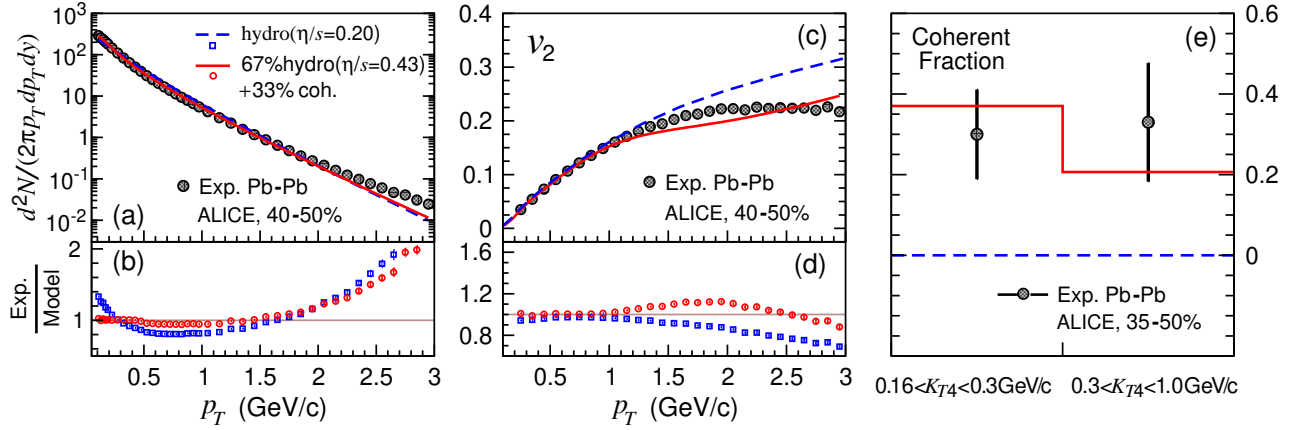


FIG. 3: (Color online) Comparison of the results of pion transverse-momentum spectrum (left panels), elliptic flow (middle panels), and coherent fraction (right panel) of the hydrodynamic chaotic source and the partially coherent source with the experimental data of pion transverse-momentum spectrum [5], elliptic flow [8], and the coherent fraction in the two K_{T4} regions, $0.16 < K_{T4} < 0.3$ GeV/c and $0.3 < K_{T4} < 1$ GeV/c [23], measured by the ALICE Collaboration in the Pb-Pb collisions at $\sqrt{s_{NN}} = 2.76$ TeV and in the centrality regions of 40–50% (left and middle panels) and 35–50% (right panel). The error bars of the experimental data of pion transverse-momentum spectrum and elliptic flow are smaller than the symbol size and hardly to observe. Quantity K_{T4} is the four-pion average transverse momentum defined as $K_{T4} = \frac{1}{4}|\mathbf{p}_{T,1} + \mathbf{p}_{T,2} + \mathbf{p}_{T,3} + \mathbf{p}_{T,4}|$.

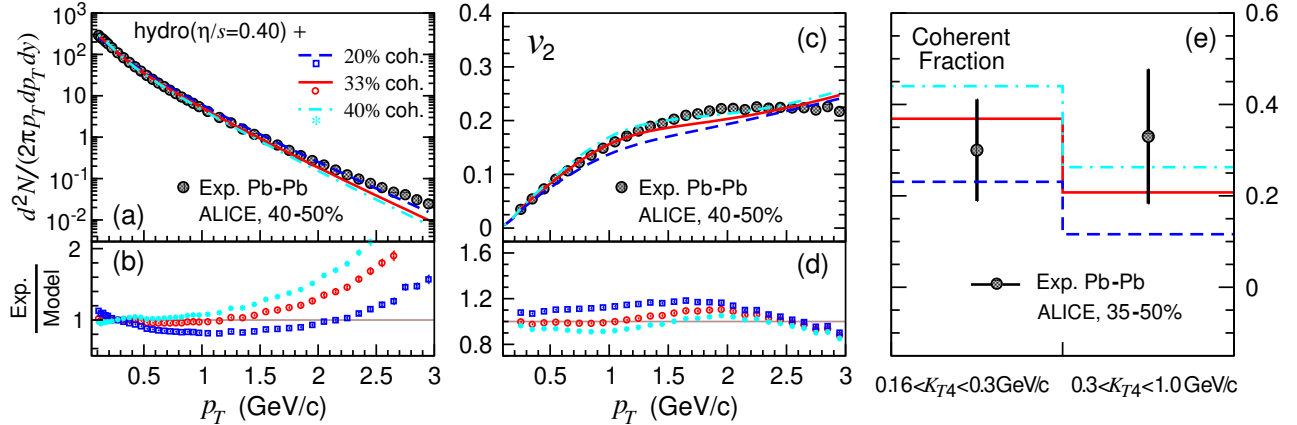


FIG. 4: (Color online) Comparison of the results of pion transverse-momentum spectrum (left panels), elliptic flow (middle panels), and coherent fraction (right panel) of the partially coherent sources, which have different total fractions of coherent emission, with the experimental data of pion transverse-momentum spectrum [5], elliptic flow [8], and the coherent fraction in the two K_{T4} regions, $0.16 < K_{T4} < 0.3$ GeV/c and $0.3 < K_{T4} < 1$ GeV/c [23]. The experimental data are measured by the ALICE Collaboration in the Pb-Pb collisions at $\sqrt{s_{NN}} = 2.76$ TeV and in the centrality regions of 40–50% (left and middle panels) and 35–50% (right panel). Quantity K_{T4} is the four-pion average transverse momentum defined as $K_{T4} = \frac{1}{4}|\mathbf{p}_{T,1} + \mathbf{p}_{T,2} + \mathbf{p}_{T,3} + \mathbf{p}_{T,4}|$.

spectrum [5] and elliptic flow [8] in the Pb-Pb collisions at $\sqrt{s_{NN}} = 2.76$ TeV and in 40–50% centrality region measured by the ALICE collaboration. We also show in the left- and middle-bottom panels of Fig. 3 the ratios of the experimental data to the results of the hydrodynamic chaotic source and the partially coherent source. One can observe that the results of the transverse-momentum spectrum and elliptic flow of the partially coherent source are a little more consistent with the experimental data than those of the hydrodynamic source.

In the right panel of Fig. 3 we show the coherent fraction of the partially coherent source and the results extracted from the

experimental measurements of four-pion Bose-Einstein correlations in the two K_{T4} regions, $0.16 < K_{T4} < 0.3$ GeV and $0.3 < K_{T4} < 1.0$ GeV, in the Pb-Pb collisions at $\sqrt{s_{NN}} = 2.76$ TeV and in 35–50% centrality region [23], where K_{T4} is the four-pion average transverse momentum defined as $K_{T4} = \frac{1}{4}|\mathbf{p}_{T,1} + \mathbf{p}_{T,2} + \mathbf{p}_{T,3} + \mathbf{p}_{T,4}|$. The coherent fraction of the hydrodynamic source is zero. However, the results of the partially coherent source are consistent with the experimental data. Because the coherent emission decreases with increasing particle momentum approximately in Gaussian formula, and the chaotic emission is approximately in Boltzmann dis-

tribution, the coherent fraction is smaller in the higher average momentum region than that in the lower average momentum region for the partially coherent source.

We further investigate the variations of pion transverse-momentum spectrum and elliptic flow of the partially coherent sources with different total fractions of coherent emission and show the results in Fig. 4 left and middle panels. Here the η/s is taken to be 0.4 for all the cases of fraction values. In Fig. 4 right panel we show the coherent fractions of the partially coherent sources in the two K_{T4} region, $0.16 < K_{T4} < 0.3$ GeV/c and $0.3 < K_{T4} < 1$ GeV/c. The experimental data presented in Fig. 4 are the same as in Fig. 3 measured by the ALICE Collaboration. We find that the results of pion transverse-momentum spectrum and elliptic flow of the partially coherent sources are sensitive to the total fraction of coherent emission. The results corresponding to the total fraction of coherent emission, 33%, are more consistent with the experimental data of pion transverse-momentum spectrum and elliptic flow, and this fraction of coherent emission is consistent with the experimental analysis results of four-pion Bose-Einstein correlations.

V. SUMMARY AND DISCUSSION

Motivated by the recent experimental observation of the suppression of multi-pion Bose-Einstein correlations in the Pb-Pb collisions at $\sqrt{s_{NN}} = 2.76$ TeV at the LHC [22, 23], we have studied a coherent pion emission and its influences on pion transverse-momentum spectrum and elliptic anisotropy in relativistic heavy ion collisions. We have constructed a partially coherent source by combining the chaotic emission source evolving with viscous hydrodynamics and a parameterized coherent emission source. It is found that the influences

of coherent emission on pion transverse-momentum spectrum and elliptic flow are related to the initial size and shape of the coherent source. This is a quantum effect but not from the source dynamical evolution. The pion transverse-momentum spectrum and elliptic flow generated by the partially coherent source with a total fraction of coherent emission, 33%, can reproduce the experimental data of the spectrum [5] and elliptic flow [8] in the Pb-Pb collisions with 40–50% centrality at the LHC. This coherent fraction is consistent with the experimental analysis results of four-pion Bose-Einstein correlations [23]. And, the small initial transverse radius of the coherent source, $R_T = 0.25$ fm, is consistent with the experimental observation, that “ The suppression observed in this analysis appears to extend at least up to $p_T \sim 340$ MeV/c. ” [23].

In relativistic heavy-ion collisions, viscous hydrodynamics has been widely used to describe the source evolution. One of the fundamental assumptions of hydrodynamics is local thermal equilibrium. So, the particle emission from the hydrodynamic evolving source is chaotic emission. Although there are some indications of coherent particle emission, its mechanism is not clear so far. The coherent part of the partially coherent source considered in this paper is a simple one. There is still a long way to go to study systematically the effect of coherence emission on experimental observables and to understand the mechanisms of coherent emission in relativistic heavy-ion collisions.

Acknowledgments

This research was supported by the National Natural Science Foundation of China under Grant Nos. 11675034 and 11275037.

-
- [1] J. Adams *et al.* (STAR Collaboration), Phys. Rev. Lett. **92**, 112301 (2004).
 - [2] S. S. Adler *et al.* (PHENIX Collaboration), Phys. Rev. C **69**, 034909 (2004).
 - [3] B. B. Back *et al.* (PHOBOS Collaboration), Phys. Rev. C **75**, 024910 (2007).
 - [4] B. Abelev *et al.* [ALICE Collaboration], Phys. Rev. Lett. **109**, 252301 (2012).
 - [5] B. Abelev *et al.* [ALICE Collaboration], Phys. Rev. C **88**, 044910 (2013).
 - [6] J. Adams *et al.* (STAR Collaboration), Phys. Rev. C **72**, 014904 (2005).
 - [7] S. Afanasiev *et al.* (PHENIX Collaboration), Phys. Rev. C **80**, 024909 (2009).
 - [8] B. B. Abelev *et al.* [ALICE Collaboration], JHEP **1506**, 190 (2015).
 - [9] U. Heinz, Landolt-Bornstein **23**, 240 (2010).
 - [10] J. Y. Ollitrault, Phys. Rev. D **46**, 229 (1992).
 - [11] B. Schenke, J. Phys. G **38**, 124009 (2011)
 - [12] R. Snellings, J. Phys. G **41**, 124007 (2014)
 - [13] H. Song, Ph.D thesis, Ohio State University, 2009, arXiv:0908.3656 [nucl-th].
 - [14] H. Song and U. Heinz, Phys. Lett. B **658**, 279 (2008).
 - [15] B. Schenke, S. Jeon and C. Gale, Phys. Rev. Lett. **106**, 042301 (2011).
 - [16] C. Gale, S. Jeon, B. Schenke, P. Tribedy and R. Venugopalan, Phys. Rev. Lett. **110**, 012302 (2013).
 - [17] C. Shen, U. Heinz, P. Huovinen and H. Song, Phys. Rev. C **84**, 044903 (2011).
 - [18] H. Song, S. Bass and U. Heinz, Phys. Rev. C **89**, 034919 (2014).
 - [19] C. Shen and U. Heinz, Nucl. Phys. News **25**, 6 (2015).
 - [20] D. Molnar, F. Wang, and C. H. Greene, arXiv:1404.4119.
 - [21] L. He, T. Edmonds, Z.-W. Lin, Feng Liu, D. Molnara, F. Wang, Phys. Lett. B **753**, 506 (2016).
 - [22] B. B. Abelev *et al.* [ALICE Collaboration], Phys. Rev. C **89**, 024911 (2014).
 - [23] J. Adam *et al.* [ALICE Collaboration], Phys. Rev. C **93**, 054908 (2016).
 - [24] C. Y. Wong, W. N. Zhang, Phys. Rev. C **76**, 034905 (2007).
 - [25] J. Liu, P. Ru, W. N. Zhang, C. Y. Wong, Int. J. Mod. Phys. E **22**, 1350083 (2013).
 - [26] J. Liu, P. Ru, W. N. Zhang, C. Y. Wong, J. Phys. G **41**, 125101 (2014).
 - [27] D. Gangadharan, Phys. Rev. C **92**, 014902 (2015).

- [28] V. Begun and W. Florkowski, Phys. Rev. C **91**, 054909 (2015).
- [29] S. Pratt, Phys. Lett. B **301**, 159 (1993).
- [30] Q. H. Zhang, W. Q. Chao and C. S. Gao, Nucl. Phys. A **608**, 469 (1996).
- [31] Q. H. Zhang, W. Q. Chao and C. S. Gao, J. Phys. G **23**, 1133 (1997).
- [32] G. Amelino-Camelia, J. D. Bjorken and S. E. Larsson, Phys. Rev. D **56**, 6942 (1997).
- [33] M.M. Aggarwal *et al.* (WA98 Collaboration), Phys. Lett. B **420**, 169 (1998).
- [34] J. P. Blaizot, F. Gelis, J. F. Liao, L. McLerran and R. Venugopalan, Nucl. Phys. A **873**, 68 (2012).
- [35] Z. Xu, K. Zhou, P. Zhuang and C. Greiner, Phys. Rev. Lett. **114**, 182301 (2015).
- [36] X. G. Huang and J. Liao, Phys. Rev. D **91**, 116012 (2015).
- [37] A. Kovner, L. D. McLerran and H. Weigert, Phys. Rev. D **52**, 6231 (1995).
- [38] E. Iancu, A. Leonidov and L. McLerran, hep-ph/0202270.
- [39] B. Schenke, S. Schlichting, P. Tribedy and R. Venugopalan, Phys. Rev. Lett. **117**, 162301 (2016).
- [40] M. H. Anderson, J. R. Ensher, M. R. Matthews, C. E. Wieman and E. A. Cornell, Science **269**, 198 (1995).
- [41] K. B. Davis, M. O. Mewes, M. R. Andrews, N. J. van Druten, D. S. Durfee, D. M. Kurn and W. Ketterle, Phys. Rev. Lett. **75**, 3969 (1995).
- [42] R. J. Glauber, Phys. Rev. **84**, 395 (1951).
- [43] R. J. Glauber, Phys. Rev. Lett. **10**, 84 (1963).
- [44] R. J. Glauber, Phys. Rev. **130**, 2529 (1963).
- [45] R. J. Glauber, Phys. Rev. **131**, 2766 (1963).
- [46] M. Gyulassy, S. K. Kauffmann and L. W. Wilson, Phys. Rev. C **20**, 2267 (1979).
- [47] R. Hanbury Brown and R. Q. Twiss, Nature **178**, 1046 (1956).
- [48] G. Goldhaber, S. Goldhaber, W. Y. Lee and A. Pais, Phys. Rev. **120**, 300 (1960).
- [49] W. N. Zhang, Y. Y. Ren and C. Y. Wong, Phys. Rev. C **74**, 024908 (2006).
- [50] J. Yang, Y. Y. Ren and W. N. Zhang, Adv. High Energy Phys. **2015**, 846154 (2015).
- [51] R. J. Glauber, Nucl. Phys. A **774**, 3 (2006).
- [52] C. Y. Wong, *Introduction to High-Energy Heavy-Ion Collisions* (World Scientific, Singapore, 1994), Chapter 17.
- [53] C. Shen, Z. Qiu, H. Song, J. Bernhard, S. Bass and U. Heinz, Comput. Phys. Commun. **199**, 61 (2016); [arXiv:1409.8164 [nucl-th]].
- [54] D. Kharzeev, E. Levin and M. Nardi, Phys. Rev. C **71**, 054903 (2005).
- [55] D. Kharzeev, E. Levin and M. Nardi, Nucl. Phys. A **747**, 609 (2005).
- [56] Z. Qiu and U. Heinz, Phys. Rev. C **84**, 024911 (2011).
- [57] H. Song and U. Heinz, Phys. Rev. C **77**, 064901 (2008).
- [58] H. Song and U. Heinz, Phys. Rev. C **78**, 024902 (2008).
- [59] U. Heinz and H. Song, J. Phys. G **35**, 104126 (2008).
- [60] P. Huovinen and P. Petreczky, Nucl. Phys. A **837**, 26 (2010).
- [61] F. Cooper and G. Frye, Phys. Rev. D **10**, 186 (1974).
- [62] J. Sollfrank, P. Koch and U. Heinz, Phys. Lett. B **252**, 256 (1990).
- [63] J. Sollfrank, P. Koch and U. W. Heinz, Z. Phys. C **52**, 593 (1991).
- [64] J. Sollfrank, P. Huovinen, M. Kataja, P. V. Ruuskanen, M. Prakash and R. Venugopalan, Phys. Rev. C **55**, 392 (1997).